General Disclaimer

One or more of the Following Statements may affect this Document

- This document has been reproduced from the best copy furnished by the organizational source. It is being released in the interest of making available as much information as possible.

- This document may contain data, which exceeds the sheet parameters. It was furnished in this condition by the organizational source and is the best copy available.

- This document may contain tone-on-tone or color graphs, charts and/or pictures, which have been reproduced in black and white.

- This document is paginated as submitted by the original source.

- Portions of this document are not fully legible due to the historical nature of some of the material. However, it is the best reproduction available from the original submission.

PROPELLANT DYNAMICS IN AN AIRCRAFT-TYPE LAUNCH VEHICLE

by

Franklin T. Dodge

Luis R. Garza

FINAL REPORT

Contract NAS8-25920

Control No. DCN 1-0-75-00087(IF)

SwRI Project 02-2879

Prepared for

NATIONAL AERONAUTICS AND SPACE ADMINISTRATION

GEORGE C. MARSHALL SPACE FLIGHT CENTER

MARSHALL SPACE FLIGHT CENTER, ALABAMA 35812

July 1971

SOUTHWEST RESEARCH INSTITUTE

SAN ANTONIO HOUSTON

SOUTHWEST RESEARCH INSTITUTE
Post Office Drawer 28510, 8500 Culebra Road
San Antonio, Texas 78284

PROPELLANT DYNAMICS IN AN AIRCRAFT-TYPE LAUNCH VEHICLE

by
Franklin T. Dodge
Luis R. Garza

FINAL REPORT
Contract NAS8-25920
Control No. DCN 1-0-75-00087(IF)
SwRI Project 02-2879

Prepared for
NATIONAL AERONAUTICS AND SPACE ADMINISTRATION
GEORGE C. MARSHALL SPACE FLIGHT CENTER
MARSHALL SPACE FLIGHT CENTER, ALABAMA 35812

July 1971

Approved:

H. Norman Abramson, Director
Department of Mechanical Sciences

ABSTRACT

Propellant sloshing in a tilted cylindrical tank is studied experimentally and analytically. Two distinct fundamental modes are shown to exist, one of which can be excited by tank motions parallel to the long axis (the "long" mode) of the elliptical free surface and one by motions perpendicular to it (the "short" mode). Experimental results show that the natural frequencies of both modes decrease as the tilt increases and the slosh damping decreases markedly with increased tilt for the long mode. The shape of the long mode is significantly asymmetrical although the short mode appears similar to the slosh mode in an upright tank. Analytical results confirm these observations, and a mathematically equivalent mechanical model is derived from the theory. The model shows that the slosh mass for the long mode decreases as the tilt increases. More importantly, the model indicates that an oscillating force is created parallel to the thrust; this could be important in POGO applications.

TABLE OF CONTENTS

LIST OF ILLUSTRATIONS

I. INTRODUCTION

Since nearly all previous rocket vehicles of interest have had axisymmetric tanks and thrust vectors parallel to the tank axis, propellant dynamics in axisymmetric tanks accelerated parallel to their axes have been studied extensively. The space shuttle now under development not only contains propellant tanks shaped to fit in an aircraft-type structural envelope but also must be controllable in horizontal flight and during the transition from vertical to horizontal flight. Thus, the tanks for the shuttle will not all be axisymmetric nor will the thrust vector always be parallel to the axes of the tanks that are axisymmetric. The research program described herein was addressed to the latter problem: determining the propellant slosh characteristics for an axisymmetric cylindrical tank when the acceleration vector is not parallel to the tank axis.

Little previous work has been devoted to the problem of sloshing in a "tilted" cylindrical tank. Bugg[1]* at NASA-MSFC experimentally determined the natural frequencies as a function of angle of tilt and liquid depth, and McNeill and Lamb[2] and Moiseev and Petrov[3] determined the slosh frequencies analytically, for cases when the free surface did not intersect the tank bottom. Chu solved a similar problem for a two-dimensional tank, by numerical methods.[4] In none of these studies were the slosh forces or moments evaluated. Consequently, an equivalent mechanical model for use in control or loads analyses has not been formulated previously.

The objectives of the present research, then, were to conduct careful experimental measurements of the frequencies, forces, and moments for sloshing in a tilted cylindrical tank, as a function of angle of tilt and liquid depth. The existing analyses were also to be extended so that an equivalent mechanical model could be developed and verified by the tests.

---

*Raised numbers in parentheses refer to references given in Section VI.

II. EXPERIMENTAL PROGRAM

The specific objectives of this part of the program were to measure the slosh forces and moments as a function of excitation frequency, for angles of tilt of 0°, 5°, 10°, 15°, and 20° and for liquid depths of 0.5, 0.75, and 1.07 times the tank diameter. For each tilt angle and liquid depth, these slosh characteristics were to be determined for both the "long" mode (excitation parallel to the major axis of the elliptical free surface) and the "short" mode (excitation parallel to the minor axis); the two modes are sketched in Figure 1.

The tank used in the tests was an aluminum right-circular cylinder, 17.75-in. inside diameter and 36 in. tall. As shown in Figure 2, a rectangular frame held the tank in place in the dynamometer arms of the SwRI Slosh Test Facility, which is a large shake table driven by a variable speed electric motor and eccentric driver-crank linkage. The tank could be positioned in the frame so that it tilted either in the direction parallel to the shake table displacement or at right angles to it. For all the tests, the shake table displacement was 0.01775 in. (0.1 percent of the tank diameter).

A strain-gage dynamometer sensed both the slosh force parallel to the horizontal excitation and the slosh moment about the axis of the dynamometer. Although the slosh force was recorded for all tests, the slosh moment was recorded only for the h/d = 1.07 tests, since these were the only tests for which the center-of-mass of the liquid coincided with the dynamometer axis. To measure the moments for the smaller depths would have required a vertical shifting of the tank and the supporting frame, a procedure that was deemed to be too time-consuming for the value of the data obtained thereby.

Figure 3 shows a typical plot of force and moment data. In this case, three resonances (at about 1.4, 2.4, and 2.7 cps) were identified. Only the first resonance was studied in detail. (The moments for the two higher frequency modes were even smaller in comparison to the first mode response than were the forces.)

Since the damping was small, various large-amplitude nonlinearities were observed around resonance in nearly every test. For the short mode tests, swirling or oscillation of the nodal line was evident, which also occurred for the small angles of tilt with the long mode tests, but, for the large angle tests of the long mode, these kinds of nonlinearities were not so prominent except for a tendency of the wave to "break."

The slosh damping was determined by measuring the decay of the slosh force after "quick-stopping" the tank. Since nonlinearities prevented measurements exactly at the resonant frequency, the slosh decay was measured just off resonance. This procedure is accurate enough for most purposes, especially if the first two or three decay cycles are neglected in computing the logarithmic

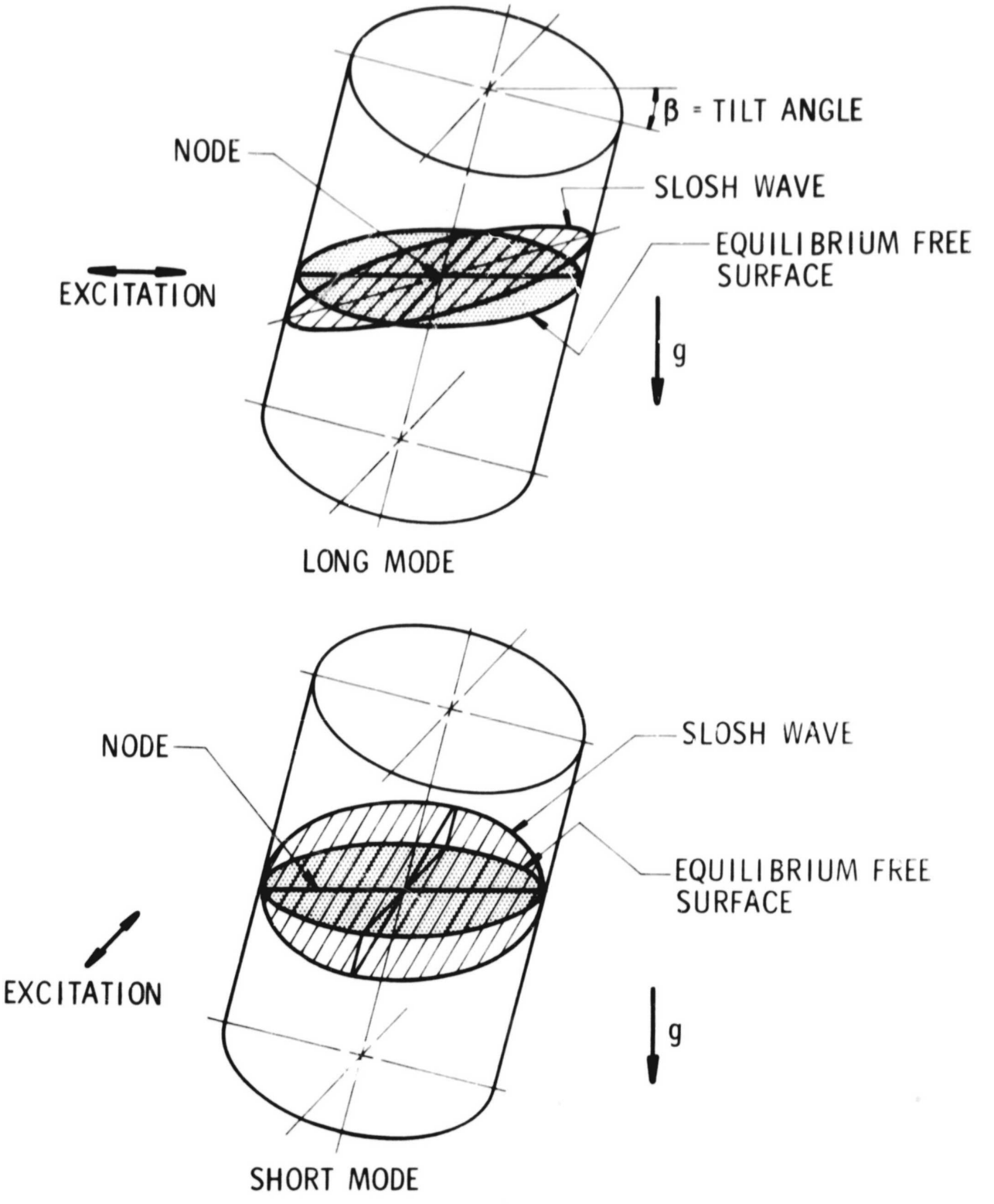

FIGURE 1. SCHEMATIC OF "LONG" AND "SHORT" MODES

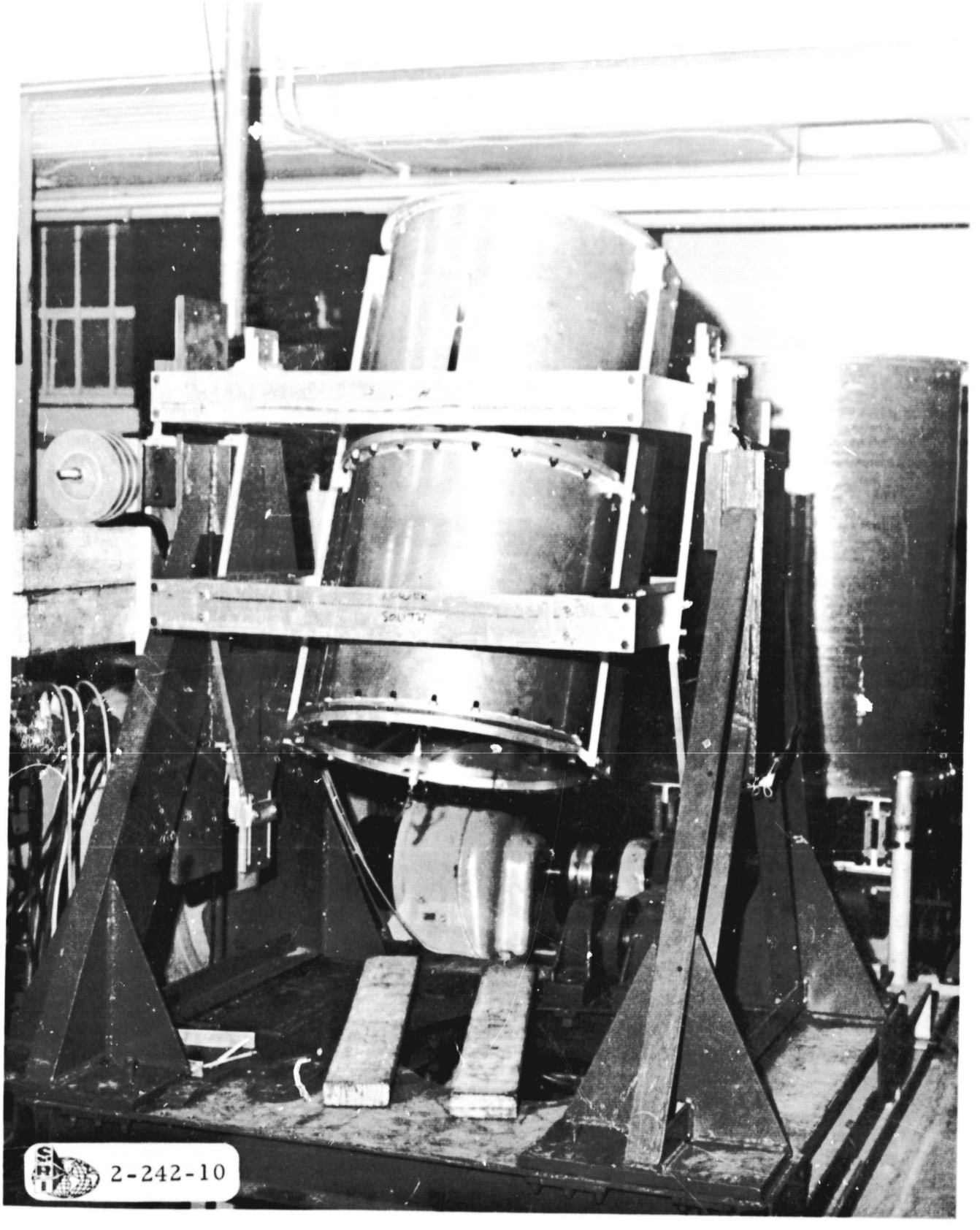

FIGURE 2. TILTED TANK INSTALLED IN SwRI SLOSH FACILITY

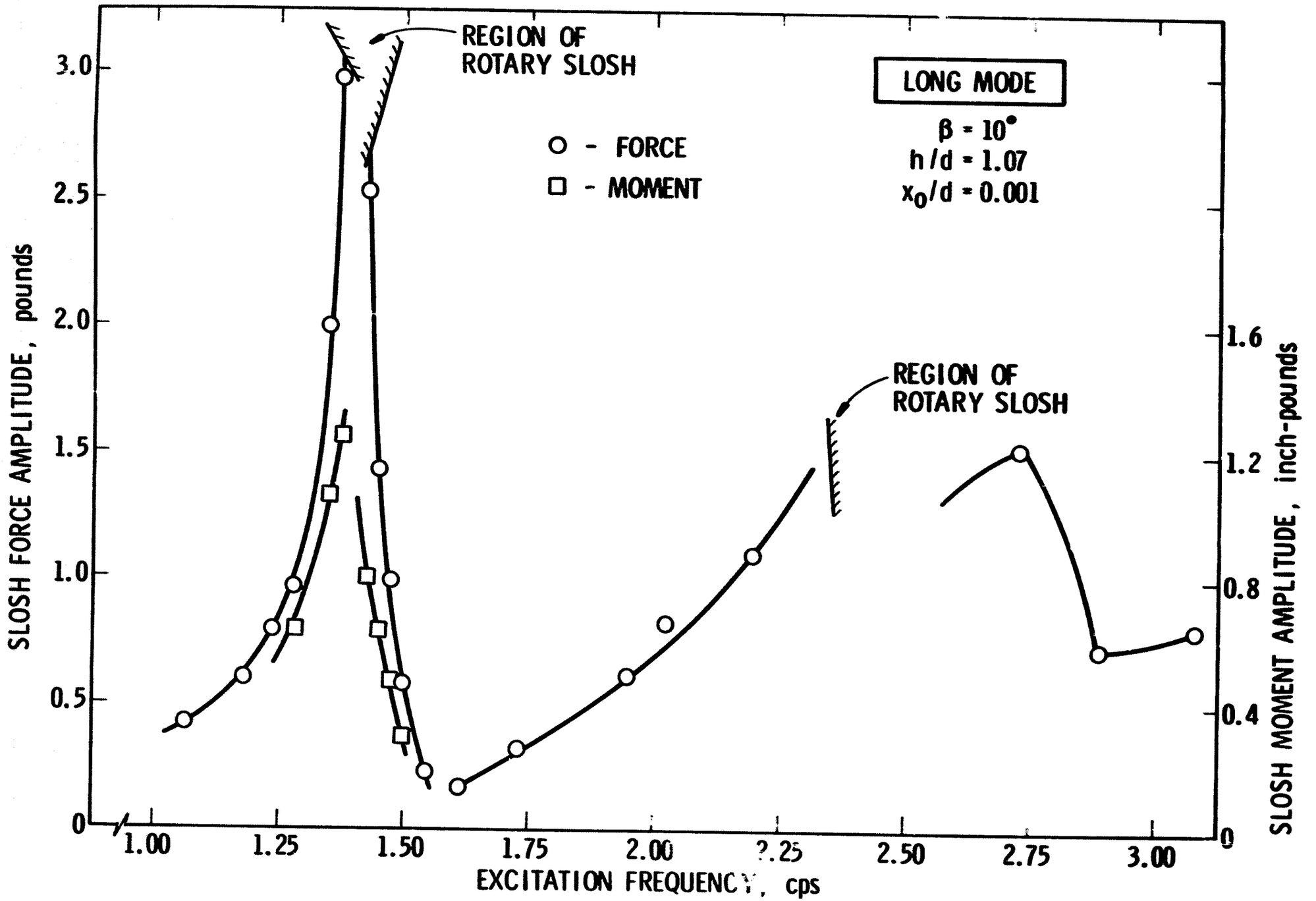

FIGURE 3. TYPICAL SLOSH FORCE AND MOMENT RESPONSE

decrements. Figure 4 shows a plot of the damping data. As the angle of tilt increases, there is a definite decrease in damping for the long mode--almost 50 percent for a tilt of 20°. No pronounced change in damping occurs for the short mode. The two flagged points on the plots are believed to be erroneous and are neglected; this is reasonable since all the damping values for a 0° tilt except the flagged $h/d = 0.75$ point agree with the published data.[5]

Qualitatively, the free surface wave shapes for the short mode resembled quite closely the waves for sloshing in an upright tank. The wave shape for the long mode, however, was skewed in such a way that the wave amplitudes near the wall where the liquid depth was greatest were much larger than the amplitudes near the other wall. Figure 5 shows a plot of the measured wave shape, compared to the predictions of a theory that will be described in the next section of the report. It can also be seen that the amplitude on the "shallow" side of the tank is greatest somewhat away from the wall, which is in contrast to sloshing in an upright tank.

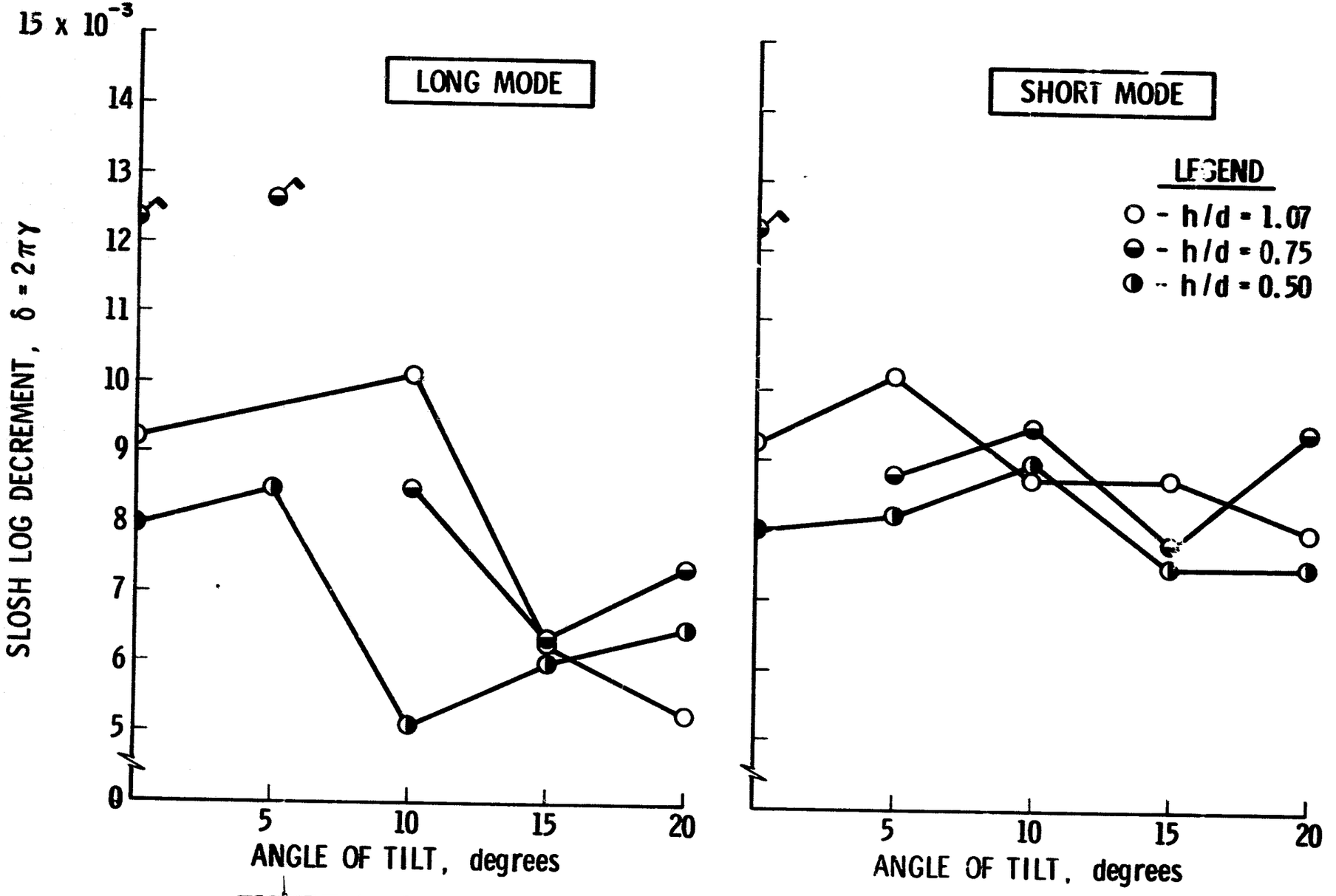

FIGURE 4. SLOSH DAMPING VARIATION WITH ANGLE OF TILT

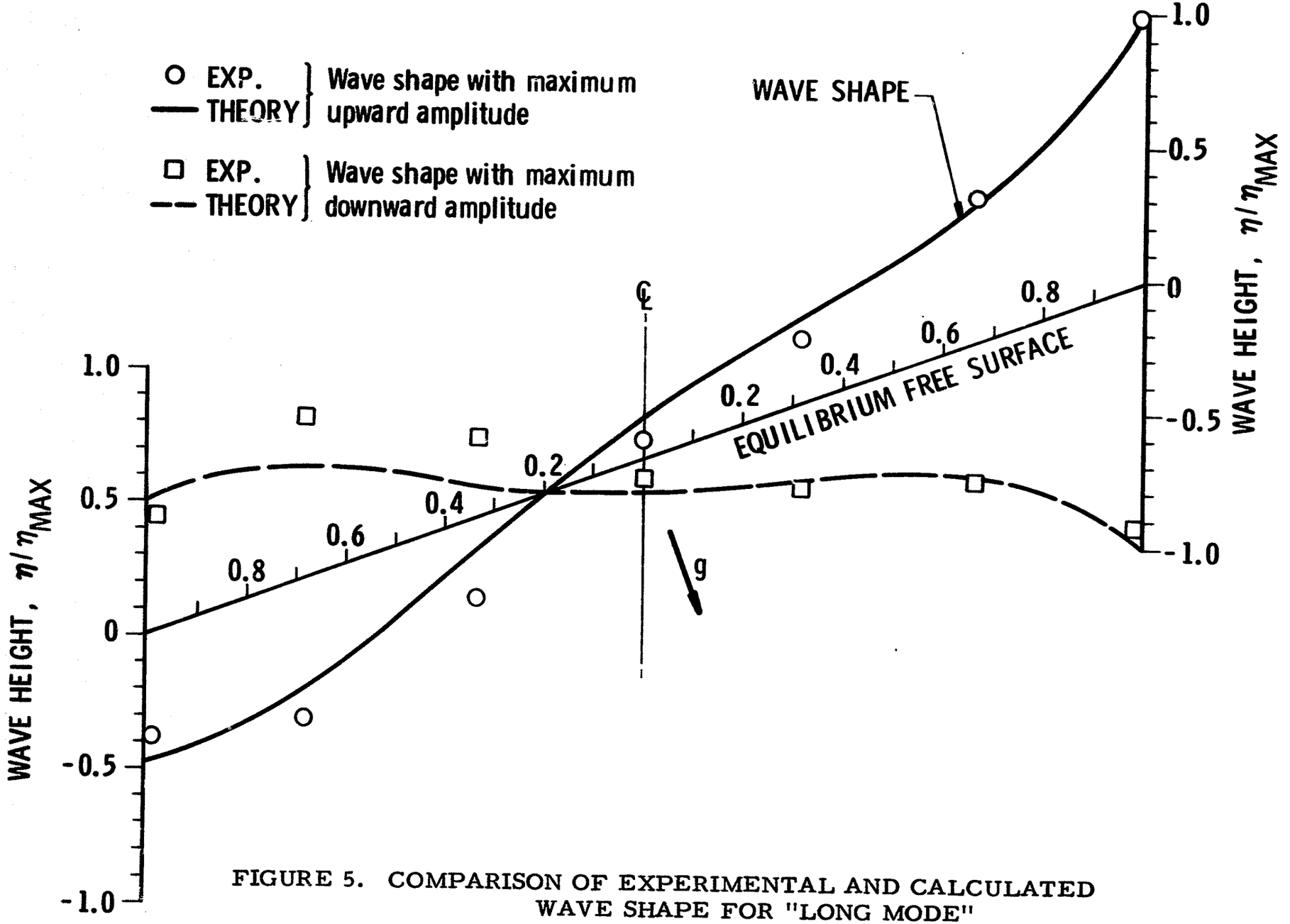

FIGURE 5. COMPARISON OF EXPERIMENTAL AND CALCULATED WAVE SHAPE FOR "LONG MODE"

III. THEORY

In this section, an analysis of sloshing in a tilted cylindrical tank is presented. The approach is similar to that outlined by Moiseev and Petrov.[3] In Section IV, the equivalent mechanical model developed from the theory is compared to the experimental measurements.

A. Velocity Potential for Free Vibrations

In order to compute the response of the liquid to various kinds of tank motions, the characteristics of the nonforced sloshing waves, or the normal modes, must be known.

Figure 6 shows the physical situation schematically. An r, θ, z coordinate system is fixed at the intersection of the tank axis and the free surface; the r-axis lies in the plane perpendicular to the tank axis. The wave height η is measured with respect to the equilibrium free surface and in a direction parallel to the z-axis. By assuming that the flow is irrotational and inviscid, a velocity potential ϕ can be used to derive the fluid velocities.

Each of the normal modes is a free vibration at the natural frequency; that is, the potential of the ith mode is $\phi_i(r, \theta, z)\cos \omega_i t$, and the corresponding wave shape is $\eta_i(r,\theta, z)\sin \omega_i t$. The linearized equations that determine ϕ_i and η_i are given below.[5]

- Conservation of mass in the fluid:

$$\nabla^2\phi_i = \frac{1}{r}\frac{\partial}{\partial r}\left(r\frac{\partial\phi_i}{\partial r}\right) + \frac{1}{r^2}\frac{\partial^2\phi_i}{\partial\theta^2} + \frac{\partial^2\phi_i}{\partial z^2} = 0 \qquad (1)$$

- Requirement of zero velocity at tank walls:

$$\frac{\partial\phi_i}{\partial r} = 0 \quad \text{at} \quad r = R_o \qquad (2)$$

$$\frac{\partial\phi_i}{\partial z} = 0 \quad \text{at} \quad z = -h \qquad (3)$$

- Relation between wave height and unsteady pressure at the free surface:

$$-\omega_i\phi_i + (g\cos\beta)\eta_i = 0 \quad \text{for} \quad z = r\cos\theta\tan\beta \qquad (4)$$

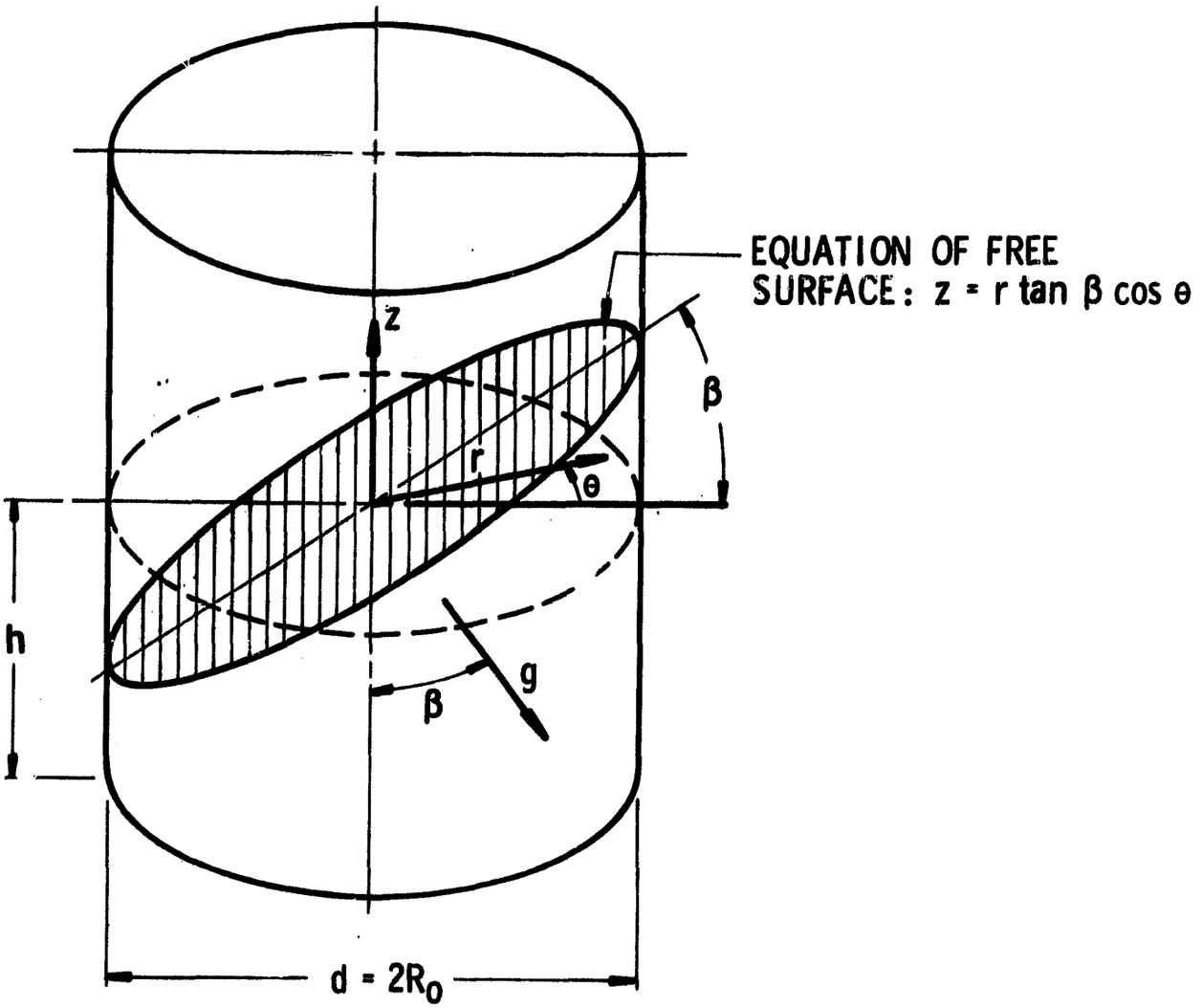

FIGURE 6. NOMENCLATURE FOR ANALYSIS

. Relation between wave height and fluid velocity:

$$\omega_i \eta_i = \frac{1}{\cos \beta} \left(\frac{\partial \phi_i}{\partial n} \right)$$

$$= \frac{1}{\cos \beta} \left(\frac{\partial \phi_i}{\partial z} \cos \beta - \frac{\sigma \phi_i}{\partial r} \sin \beta \cos \theta - \frac{\partial \phi_i}{r \partial \theta} \sin \beta \sin \theta \right)$$

$$\text{for} \quad z = r \cos \theta \tan \beta \tag{5}$$

In Equation (5), $\partial \phi_i / \partial n$ is the fluid velocity perpendicular to the free surface and involves all three vertical, radial, and tangential velocities. Equations (4) and (5) can be combined to give one equation in ϕ_i:

$$- \omega_i^2 \phi_i + g \left[\frac{\partial \phi_i}{\partial z} \cos \beta - \frac{\partial \phi_i}{\partial r} \sin \beta \cos \theta - \frac{\partial \phi_i}{r \partial \theta} \sin \beta \sin \theta \right] = 0 \tag{6}$$

$$\text{for} \quad z = r \cos \theta \tan \beta$$

Equations (1), (2), (3) and (6) completely define the velocity potential, but they cannot be solved "exactly" except for the case $\beta = 0°$. There are several ways to solve the equations approximately (or "exactly" by a limiting process), such as energy or variational methods, or expansion of ϕ_i in a power series and the determination of the coefficients by Galerkin's method, or numerical analysis. For this case, the energy method has been selected, but numerical analysis would be more appropriate for a tank of generalized shape.

Moiseev and Petrov[3], Troesch[6], Lawrence, Wang, and Reddy[7], and others have shown that minimizing the integral of the difference between the kinetic and the potential energy is the proper energy method for sloshing. That is, if the potential ϕ minimizes the integral

$$A = \frac{1}{2} \rho \int_{t_1}^{t_2} \left\{ \iint \left[\phi \frac{\partial \phi}{\partial n} - \frac{\omega^2}{g} \phi^2 \right] ds \right\} dt \tag{8}$$

and if it is also picked such that the approximating functions for ϕ satisfy Equations (1), (2), and (3), then in the limit ϕ will satisfy Equation (6) exactly. The integrals in Equation (8) are to be evaluated at the equilibrium free surface, $z = r \cos \theta \tan \beta$. Minimizing Equation (8) not only will determine all of the normal modes ϕ_i but will also determine all of the natural frequencies ω_i.

The potential ϕ is approximated as a sum of the known normal modes for an upright tank. In nondimensional coordinates, this approximation is

$$\Phi = \cos \Omega\tau \left(\sum_{k=0}^{N-1} \sum_{j=1}^{N} \frac{1}{\Lambda_{kj}} \left[J_k(\lambda_{kj} R) \right] \left\{ \frac{\cosh[\lambda_{kj}(Z + H)]}{\cosh \lambda_{kj} H} \right\} \times \left[a_{kj} \cos k\theta + \gamma_{kj} \sin k\theta \right] \right) \qquad (9)$$

where $R = r/R_o$, $Z = z/R_o$, $H = h/R_o$, $\Omega = \omega\sqrt{R_o/g}$, $\tau = t\sqrt{g/R_o}$, and $\Phi = \phi/\sqrt{gR_o^3}$. The λ_{kj} are determined by the requirement that $dJ_k/dR = 0$ at $R = 1$, which assures that each term in the series satisfies Equation (2), and the cosh $[\lambda_{kj}(Z + H)]$ function assures that each term satisfies Equation (3). Also, each term individually satisfies Equation (1). The $\Lambda_{kj} = J_k(\lambda_{kj}) \times \left\{ \pi \left[1 - \frac{k^2}{\lambda_{kj}^2} \right] / 2 \right\}^{1/2}$ are normalizing factors such that the integral over the free surface of the square of each term in the series equals one for $\beta = 0°$; this fact is a valuable check on the numerical work and computer programming. The constants a_{kj} and γ_{kj} are to be determined in such a way that Equation (8) is minimized.

After integrating over one cycle in time, Equation (8) can be written as

$$A = \frac{1}{2} \rho R_o^4 (g/R_o) \sum_{k=0}^{N-1} \sum_{j=1}^{N} \sum_{m=0}^{N-1} \sum_{\ell=1}^{N} \left\{ \left[K1_{kjm\ell} - \Omega^2 K2_{kjm\ell} \right] a_{kj} a_{m\ell} + \left[K3_{kjm\ell} - \Omega^2 K4_{kjm\ell} \right] \gamma_{kj} \gamma_{m\ell} \right\} \qquad (10)$$

The K1, K2, K3, K4 are integrals of terms such as, for example,

$$\frac{1}{\Lambda_{kj}\Lambda_{m\ell}} \int_0^1 \int_0^{2\pi} \left\{ J_k(\lambda_{kj} R) J_m(\lambda_{m\ell} R) \left(\frac{\cosh[\lambda_{kj}(R \cos\theta \tan\beta + H)]}{\cosh \lambda_{kj} H} \right) \times \left(\frac{\sinh[\lambda_{m\ell}(R \cos\theta \tan\beta + H)]}{\cosh \lambda_{kj} H} \right) \left[\cos k\theta \cos m\theta \ \underline{\text{or}} \ \sin k\theta \sin m\theta \right] \right\} R \, d\theta \, dR \qquad (11)$$

By expressing the hyperbolic cosine and sines as exponentials and using the sum and difference formulas for the products of cosines or sines, integrals such as Equation (11) can be integrated analytically over θ, with the results being given in terms of modified Bessel functions such as $I_{k \pm m} [(\lambda_{kj} \pm \lambda_{m\ell}) \times r \tan\beta]$ as explained in Reference 8. The final integration over r can be performed numerically, say by Simpson's rule.

Notice that there are no terms which involve products of cos $k\theta$ and sin $m\theta$; these terms give integrands that are an odd function of θ and therefore integrate to zero. Thus, the cosine terms correspond to the long modes, and the sine terms to the short modes.

By requiring that $\partial A/\partial a_{kj} = 0$ and $\partial A/\partial \gamma_{kj} = 0$ (which minimizes the integral), a standard eigenvalue matrix ($N^2 \times N^2$) results. The matrix has been solved numerically for a number of values of tilt angle β and depth ratio $H = h/R_o$. If $N \times N$ terms are used in Equation (9), N^2 natural frequencies and N^2 sets of a_{kj} or γ_{kj} are determined. The interest here is in only the results for the lowest frequency long mode, the lowest frequency short mode, and the corresponding sets of eigenvectors a_{kj} and γ_{kj}.

The natural frequency results are shown in Figure 7. For h/d = 1.07, the predicted frequencies are lower than the measured ones for both the long and short modes. The discrepancy is not large, and in fact is slightly less than that given by the theory of Moiseev and Petrov.[3] [No results are given by McNeill and Lamb[2] for tilt angles less than 30°.] The discrepancies for either h/d = 0.75 or 0.50 are similar; the theoretical curves for these h/d values are not shown in Figure 7 for the sake of clarity.

The magnitudes of the parameters a_{kj} and γ_{kj} in Equation (9) are shown in Figures 8a and 8b, for the fundamental modes with h/d = 1.07. The variation of these parameters for the other h/d's was similar to the presented results. In these plots, the coefficients a_{11} and γ_{11} of the predominant terms [$J_1(\lambda_{11}R) \times \cos\theta$ and $J_1(\lambda_{11}R)\sin\theta$, for the long and short modes, respectively] have been set equal to one; also, all the γ_{kj} for k = 0 are identically zero for the short mode. It can be seen that the $J_2(\lambda_{21}R)\cos 2\theta$ and $J_2(\lambda_{21}R)\sin 2\theta$ terms are the predominant disturbances for these modes; however, the distortion of the short mode (i.e., magnitude of γ_{21}) is considerably less than for the long mode. These plots indicate, furthermore, that the assumption that Φ depends only on cos θ or sin θ terms [that is, neglecting all $J_o(\lambda_{ok}R)$ and cos $m\theta$, sin $m\theta$ terms, as McNeill and Lamb[2] did] can lead to serious error.

The computed wave shape for $\beta = 20°$ and h/d = 1.07, using the values of a_{kj} presented in Figure 8, was shown previously in Figure 5. The theory predicts all the observed features very closely, as can be seen, and, in particular, it predicts the definite skewness of the wave.

B. Forced Vibrations

For forced vibrations, the governing equations are similar to the ones given previously except that the boundary conditions at the tank walls and bottom are now

$$\frac{\partial \phi}{\partial r} = x_o \omega \cos\theta \cos\beta \quad \text{for} \quad r = R_o \tag{12}$$

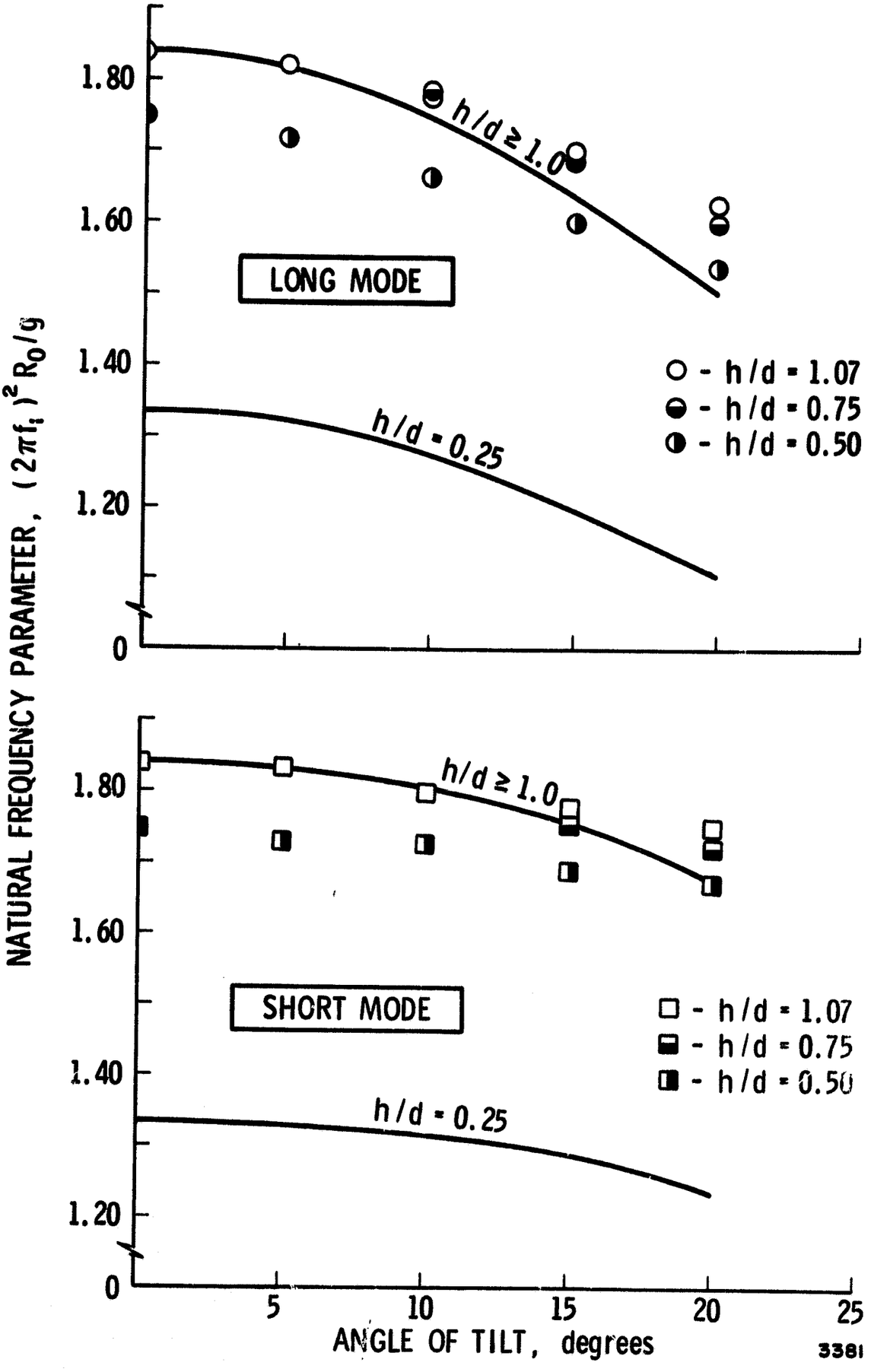

FIGURE 7. NATURAL FREQUENCY VARIATION WITH ANGLE OF TILT

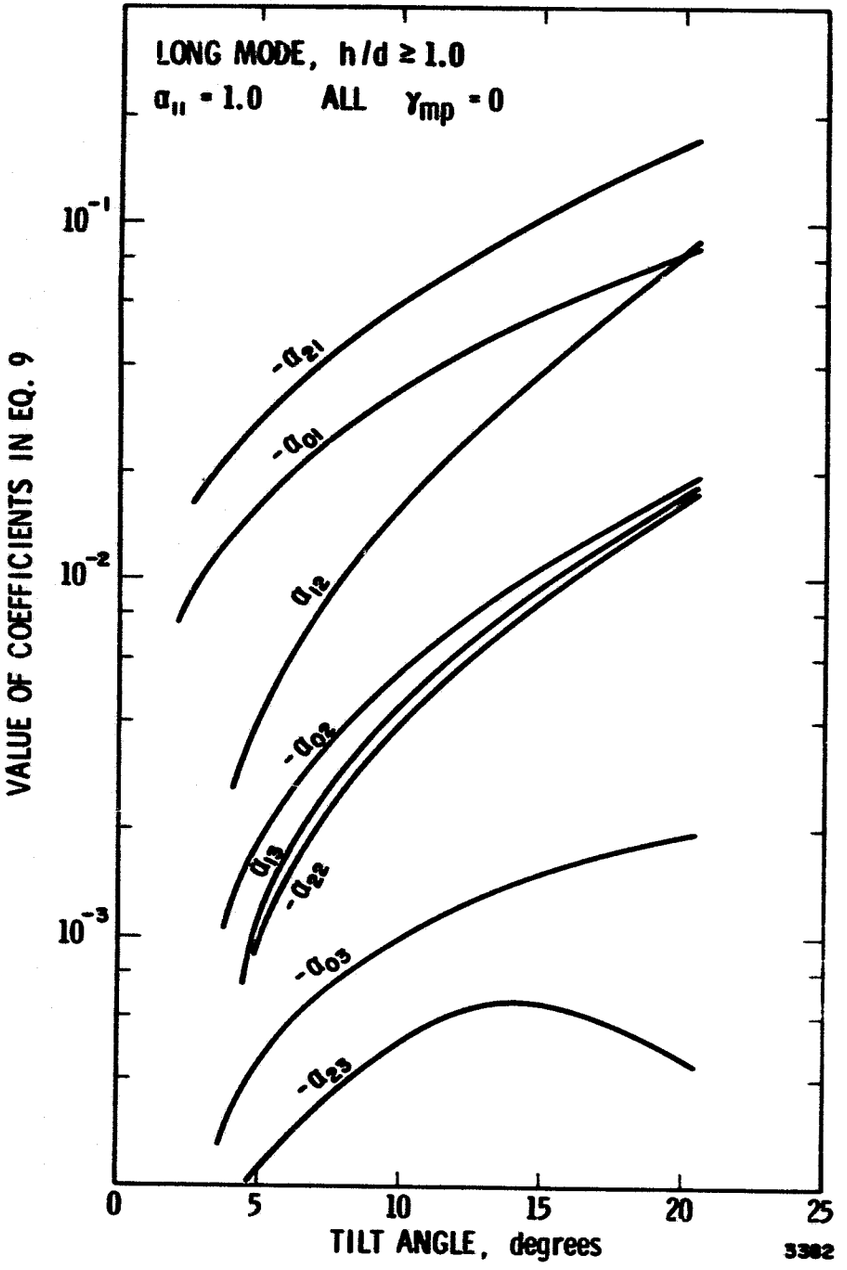

A. Long Mode

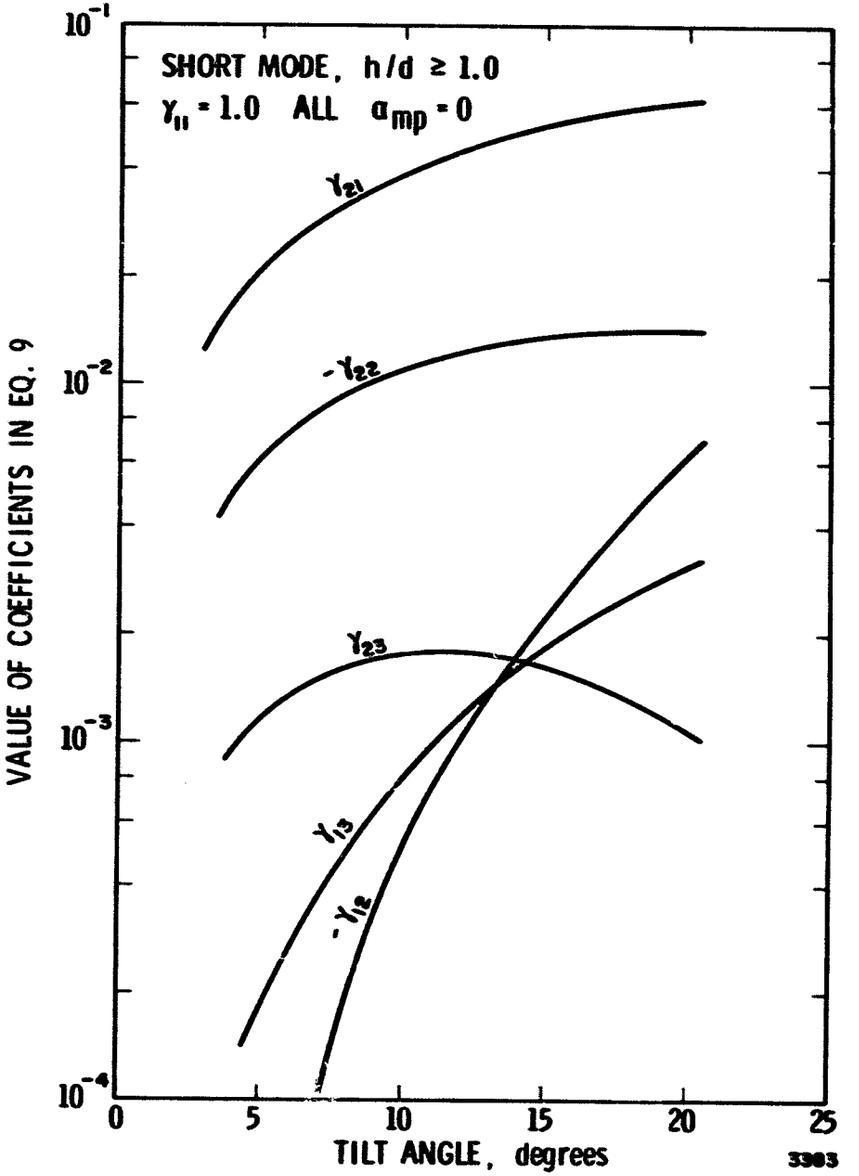

B. Short Mode

FIGURE 8. COEFFICIENTS FOR FUNDAMENTAL MODE

and

$$\frac{\partial \phi}{\partial z} = x_o \omega \sin \beta \quad \text{for} \quad z = -h \tag{13}$$

which matches the velocity of the tank walls and the fluid in contact with the walls. These equations are written for an excitation of $x_o \sin \omega t$ parallel to the major diameter of the elliptical free surface; for excitation of the short mode, the $\cos \theta$ in Equation (12) should be replaced by $\sin \theta$.

Now, a new potential $\overline{\phi}$ is introduced such that

$$\overline{\phi} \cos \omega t = \cos \omega t[\phi(r,\theta, z) - x_o \omega r \cos \theta \cos \beta - x_o \omega z \sin \beta] \tag{14}$$

Substituting this relation for ϕ into all the equations gives a set of equations for $\overline{\phi}$ that are identical to Equations (1), (2), and (3); however, Equation (6) is replaced by

$$-\omega^2 \overline{\phi} + g \left[\frac{\partial \overline{\phi}}{\partial z} \cos \beta - \frac{\partial \overline{\phi}}{\partial r} \sin \beta \cos \theta - \frac{\partial \overline{\phi}}{r \partial \theta} \sin \beta \sin \theta\right] = \frac{\omega^3 x_o r \cos \theta}{\cos \beta}$$

$$\text{for} \quad z = r \cos \theta \tan \beta \tag{15}$$

The standard procedure is to set $\overline{\phi} \cos \omega t = \left\{\sum_{i=1}^{\infty}\right\} B_i \phi_i \cos \omega t$ where the ϕ_i's are the normal modes and the B_i's are unknown coefficients. Such a series expansion for $\overline{\phi}$ automatically insures that $\overline{\phi}$ satisfies Equations (1), (2), and (3). Substituting $\overline{\phi} = \sum B_i \phi_i$ into Equation (15), and adding and subtracting the series $\sum B_i \omega_i^2 \phi_i$ gives the result that

$$\sum_{i=1}^{\infty} B_i(\omega_i^2 - \omega^2)\phi_i + \sum_{i=1}^{\infty} B_i \left\{-\omega_i^2 \phi_i + g \left[\frac{\partial \phi_i}{\partial z} \cos \beta - \frac{\partial \phi_i}{\partial r} \sin \beta \cos \theta - \frac{\partial \phi_i}{r \partial \theta} \sin \beta \sin \theta\right]\right\} = \frac{\omega^3 x_o r \cos \theta}{\cos \beta} \quad \text{for} \quad z = r \cos \theta \tan \beta \tag{16}$$

The term in braces is identically zero, since each ϕ_i satisfies Equation (6). Therefore, the constants B_i are determined from the relation

$$\sum_{i=1}^{\infty} B_i(\omega_i^2 - \omega^2)\phi_i = \frac{\omega^3 x_o r \cos \theta}{\cos \beta} \quad \text{for} \quad z = r \cos \theta \tan \beta \tag{17}$$

By using Green's theorem, it can be shown that the normal modes satisfy the orthogonality relation

$$\int_0^1 \int_0^{2\pi} \phi_m \phi_n r \, d\theta \, dr = 0 \quad \text{if} \quad m \neq n, \quad \text{for} \quad z = r \cos\theta \tan\beta \tag{18}$$

Thus, the coefficients B_i can be computed one at a time from Equation (17) by multiplying through by $\phi_i r$ and integrating

$$B_i = \frac{\omega^3 x_o}{\cos\beta(\omega_i^2 - \omega^2)} \left[\frac{\int_0^1 \int_0^{2\pi} \phi_i r^2 \cos\theta \, d\theta \, dr}{\int_0^1 \int_0^{2\pi} \phi_i^2 r \, d\theta \, dr} \right]$$

$$\text{for} \quad z = r \cos\theta \tan\beta \tag{19}$$

In particular, Equation (19) shows that the fundamental mode will predominate when the excitation frequency is near to or equals ω_1. (The integrals can be evaluated numerically.)

The forces and moments exerted on the tank walls can be evaluated in terms of the unsteady pressure, $\rho\partial\phi/\partial t$. For the long mode, as an example, the force is composed of two parts: the force normal to the cylindrical walls, which is parallel to the line $\theta = 0°$, and the force on the tank bottom, which is parallel to the z-axis. For the fundamental mode ($\overline{\phi} = B_i\phi_i$), the first part of the force is

$$F_x = \rho \int_0^{2\pi} \int_{-h}^{\cos\theta \tan\beta} \left[\omega B_1 \phi_1 (r = R_o) + \omega^2 x_o R_o \cos\theta \cos\beta + \omega^2 x_o z \sin\beta \right] \cos\theta \, R_o \, dz \, d\theta \tag{20}$$

Simplifying Equation (20) gives

$$F_x = (\pi\rho R_o^2 h) x_o \omega^2 \cos\beta + \rho R_o B_1 \int_0^{2\pi} \int_{-h}^{\cos\theta \tan\beta} \times \phi_1 (r = R_o) \cos\theta \, dz \, d\theta \tag{21}$$

where $\pi\rho R_o^2 h = m_t$ is the total liquid mass in the tank. Likewise, the axial part of the force parallel to the z-axis is

$$F_z = (\pi\rho R_o^2 h)x_o\omega^2 \sin\beta - \rho R_o \omega B_1 \int_0^{2\pi}\int_0^1 \phi_1(z = -h) r\, dr\, d\theta \qquad (22)$$

The last integral in Equation (22) is exactly zero, since all the terms proportional to cos $m\theta$ (or sin $m\theta$) give zero when integrated over θ from 0 to 2π, and the terms independent of θ (the J_0 terms) integrate over r to give zero.

The net horizontal force parallel to the excitation is

$$F_{horiz} = F_x \cos\beta + F_z \sin\beta = (\pi\rho R_o^2 h)(\cos^2\beta + \sin^2\beta)x_o\omega^2$$

$$+ \rho R_o \omega B_1 \cos\beta \int_0^{2\pi}\int_{-h}^{\cos\theta\tan\beta} \phi_1(r = R_o)\cos\theta\, dz\, d\theta \qquad (23)$$

The net vertical force (parallel to the thrust axis) is

$$F_{vert} = F_z \cos\beta - F_x \sin\beta = (\pi\rho R_o^2 h)(\cos\beta\sin\beta - \sin\beta\cos\beta)x_o\omega^2$$

$$- \rho R_o \omega B_1 \sin\beta \int_0^{2\pi}\int_{-h}^{\cos\theta\tan\beta} \phi_1(r = R_o)\cos\theta\, dz\, d\theta \qquad (24)$$

Substituting for B_1 in these equations gives

$$F_{horiz} = m_T x_o\omega^2 + m_T x_o\omega^2 \left(\frac{R_o}{h}\right)\left(\frac{\omega^2 x_o}{\omega_1^2 - \omega^2}\right)\mathcal{Q}$$

$$F_{vert} = -m_T x_o\omega^2 \left(\frac{R_o}{h}\right)\left(\frac{\omega^2 x_o}{\omega_1^2 - \omega^2}\right)\mathcal{Q}\tan\beta \qquad (25)$$

where $\mathcal{Q}$ is the product of the integrals in Equation (19) (which defines B_1) and Equations (24) or (25), divided by π.

The striking thing about these results is that a <u>horizontal</u> acceleration of the tank induces a <u>vertical</u> force that is proportional to the horizonal force multiplied by tangent of the angle of tilting of the tank. This oscillating force in the direction of the thrust vector may have important consequences in the POGO problem.

The slosh moments can be computed similarly, as can the forces and moments for the short mode.

IV. MECHANICAL MODEL

The parameters for an equivalent (mathematical) mechanical model can be derived either from the analysis given in Section III or from the tests described in Section II. Such a mechanical model, which duplicates the slosh forces and moments, is shown in Figure 9.

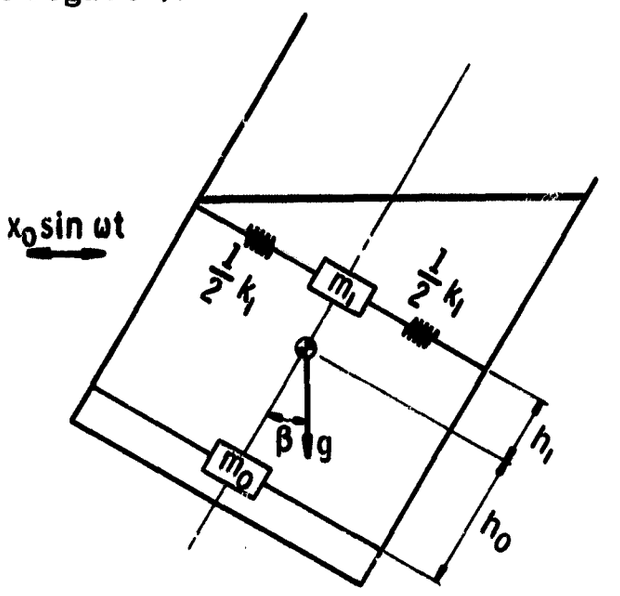

FIGURE 9. EQUIVALENT MECHANICAL MODEL

The amplitude of the horizontal force exerted on the tank by the mechanical model is

$$F_{horiz} = \omega^2 x_o \left[(m_o + m_1) + m_1 \cos^2\beta \left(\frac{\omega^2}{\omega_1^2 - \omega^2} \right) \right] \tag{26}$$

and the vertical force is

$$F_{vert} = -\omega^2 x_o \tan\beta \left[m_1 \cos^2\beta \left(\frac{\omega^2}{\omega_1^2 - \omega^2} \right) \right] \tag{27}$$

(There is also a static force that is related only to the angle of tilt; this force is also in the fluid dynamic analysis but neglected in the results.)

Comparing Equations (26) and (27) with Equations (24) and (25) shows that the model will duplicate the analytically predicted force if

$$m_o + m_1 = m_T \tag{28}$$

and

$$m_1 = m_T \left(\frac{R_o}{h}\right) \mathcal{Q} / \cos^2\beta = \frac{1}{2} m_T \left(\frac{d}{h}\right) \mathcal{Q} / \cos^2\beta \qquad (29)$$

These two equations state that the total mass of the model must equal the total mass of the liquid and relate the amount of liquid that participates in the sloshing to β and h/d.

The parameters m_o, m_1, and ω_1 can also be derived from measurements of F_{horiz} versus ω, as mentioned earlier. One method of accomplishing this is to set F_{horiz} in Equation (26) equal to the experimentally determined force for a number of values of ω; this gives a set of simultaneous equations to solve for m_o, m_1, and ω_1. Figure 10 shows a plot of the variation of m_1 with β and h/d as determined by both methods. The comparison is very close, with the differences well within the limits of experimental scatter.

Perhaps surprisingly, m_1 for the long mode decreases as β increases. It might be reasoned intuitively that since tilting the tank increases the length of the free surface in the direction of the excitation, the slosh mass should increase as β increases; that is, since m_1 for an upright cylindrical tank is[5]

$$m_1 = \frac{m_T}{4.4} \left(\frac{d}{h}\right) \tanh \left(3.68 \frac{h}{d}\right) \qquad (30)$$

an increase in d should lead to an increase in m_1. The fact that m_1 actually decreases must, therefore, be related to the increasing skewness of the mode shape as β increases.

Figure 11 compares F_{horiz} as predicted by the mechanical model to that measured in the tests, for the case $\beta = 20°$ and h/d = 1.07. Again, the comparison is close. [The experimentally determined ω_1 was used in the mechanical model to construct this plot, since otherwise the small difference between this ω_1 and the theoretical ω_1 (Fig. 7) would shift the force-response to a slightly lower frequency and mask the overall good agreement in the force prediction.]

The location of m_1 in the tank (i.e., h_1) was also computed from the test data. Within the accuracy limits of the data, no difference in h_1 from its known value for $\beta = 0°$ was noticeable; therefore, these results are not presented.

Slosh damping can be inserted in the model just as for the case of an upright tank.[5]

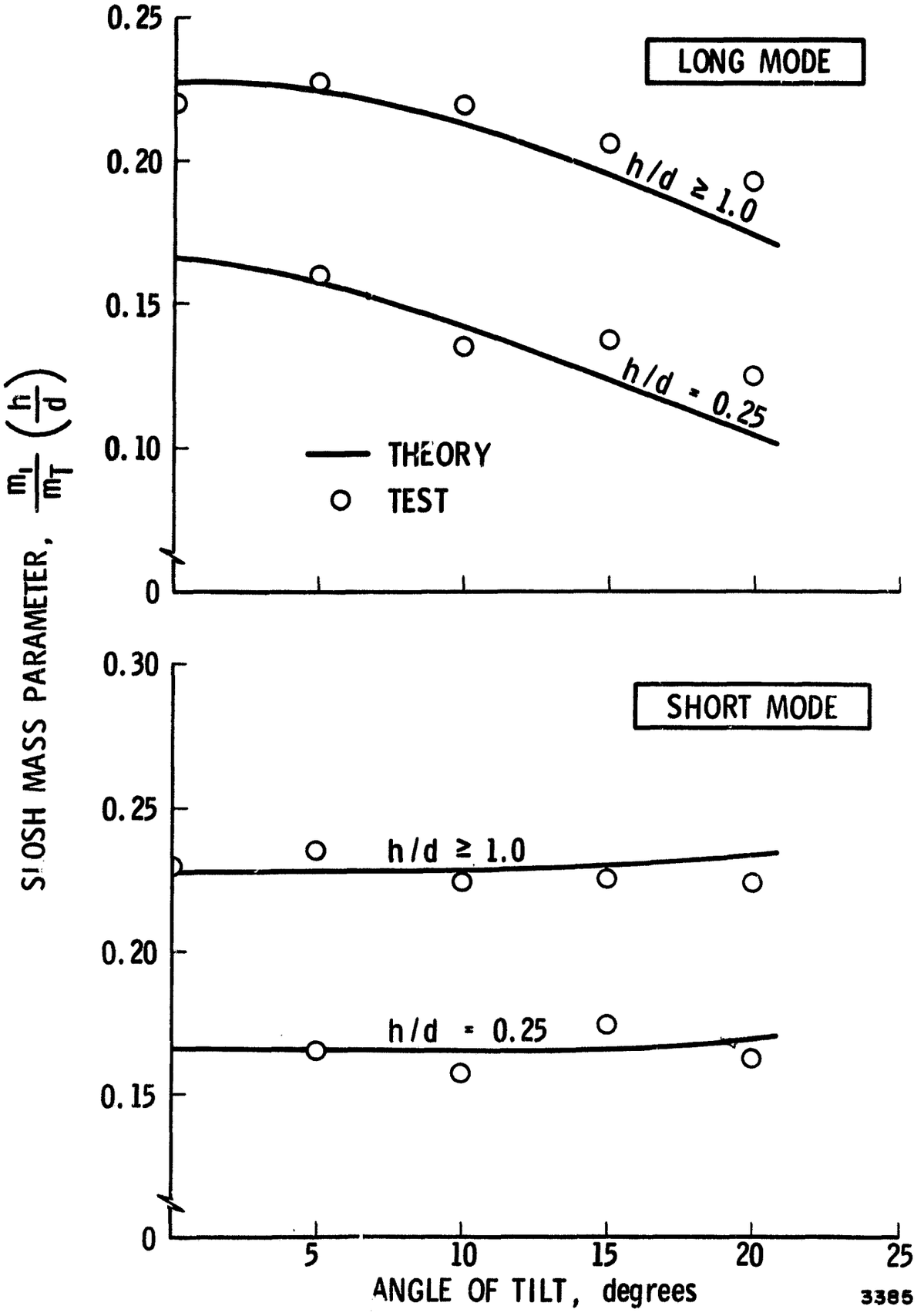

FIGURE 10. SLOSH MASS VARIATION WITH TILT ANGLE AND DEPTH RATIO

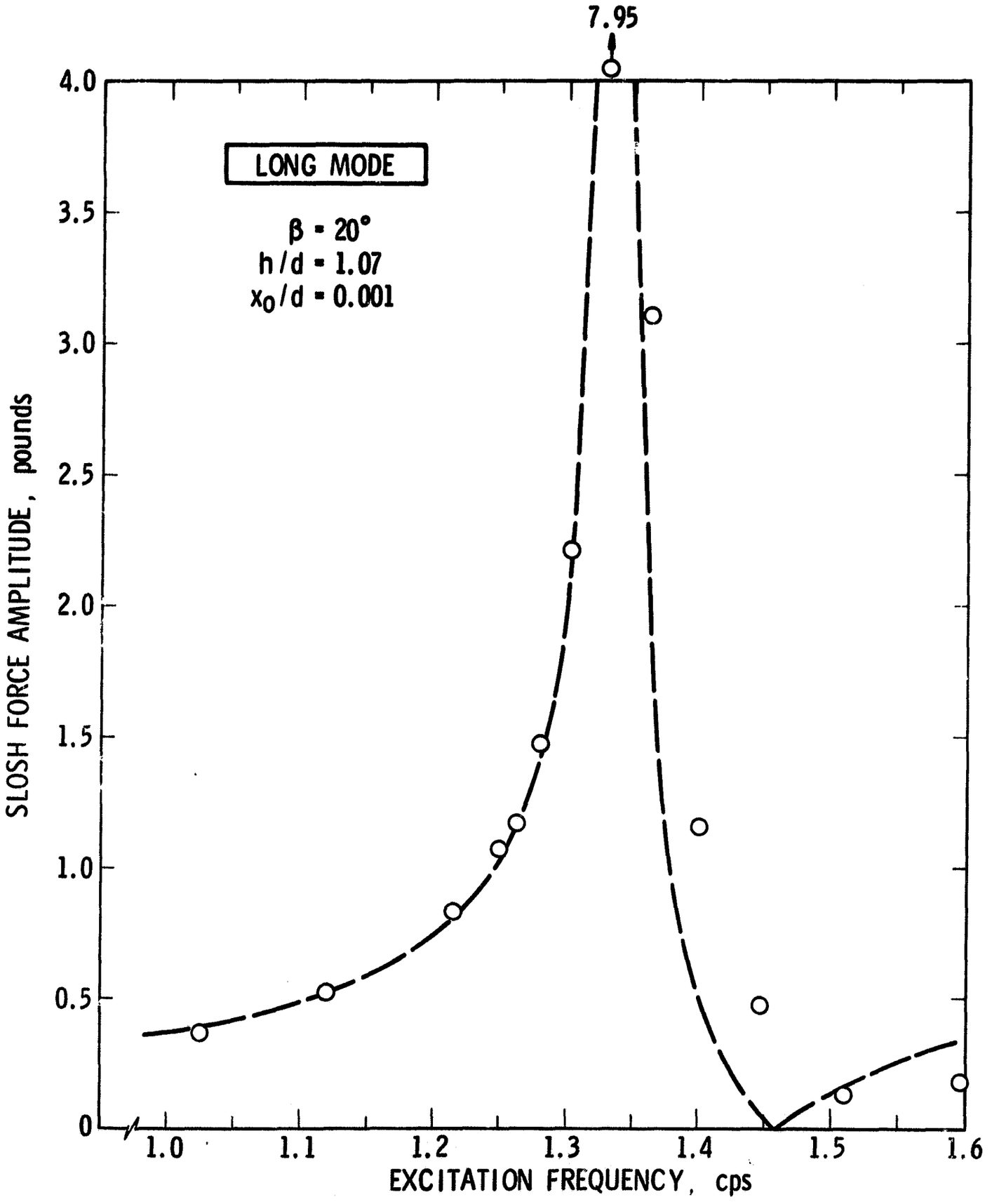

FIGURE 11. SLOSH FORCE PREDICTED BY MODEL

V. CONCLUSIONS AND RECOMMENDATIONS FOR FUTURE RESEARCH

Several interesting features of propellant dynamics in a tilted cylindrical tank were revealed by this experimental and analytical study. For example, within the range of the variables tested ($0° \leq \beta \leq 20°$, $0.5 \leq h/d \leq 1.07$), it was found experimentally that the free-surface waves become increasingly skewed as the tilt increases (see Fig. 5); the skewing is also predicted by the present fluid dynamic analysis [although some earlier analyses fail to do so[2]]. Both the theory and the tests show that for the long mode the mass of liquid participating in the sloshing decreases as the tilt increases; but, since the slosh damping also decreases as the tilt increases, the peak forces for a tilted tank are still larger than for an upright tank. On the other hand, the sloshing mass and the damping for the short mode remain relatively constant as the tilt increases. It was also found, experimentally and analytically, that the slosh resonant frequencies for both the long and short modes decrease as the tilt increases, although the decrease for the long mode is much more pronounced.

Perhaps most important of all, the theory shows that an oscillating force in the direction of the acceleration vector is created by the sloshing when the tank is tilted, and the force increases as the tilt increases. An oscillating force in the direction of the thrust can have important consequences for the POGO problem.

The research should be extended in several directions. Experimentally, larger angles of tilt should be tested to discover if the traveling-wave type of sloshing[9, 10] will be a problem for the space shuttle, and smaller liquid depths should be used in order to study the sloshing that occurs when the free surface intersects the tank bottom. Other important tank geometries besides cylindrical should be investigated. Analytically, the theory should be extended to include other tank shapes and greater variations in β and h/d; likewise, traveling-wave responses should be studied in detail. Because of its probable importance in creating POGO-type oscillations, the slosh force in the thrust direction should be investigated analytically and experimentally in much greater detail than was possible during the present program.

VI. REFERENCES

1. Bugg, F., "Experimental Determination of Liquid Oscillation Frequency in an Inclined Right Circular Cylinder," NASA TM X-64540, November 1970.

2. McNeill, W. A. and Lamb, J. P., "Fundamental Sloshing Frequency for an Inclined, Fluid-Filled Right Circular Cylinder," J. Spacecraft & Rockets, 7, August 1970, pp. 1001-1002.

3. Moiseev, N. N. and Petrov, A. A., "The Calculation of Free Oscillations of a Liquid in a Motionless Container," Advances in Applied Mechanics, Vol. 9, Academic Press (1966), pp. 91-154.

4. Chu, W. H., "Sloshing of an Arbitrary Two-Dimensional Tank with Flat Mean Free Surface," Transactions, Canadian Aeronautics and Space Institute, 4, March 1971, pp. 58-60.

5. The Dynamic Behavior of Liquids Contained in Moving Containers, H. N. Abramson (ed), NASA SP-106, 1966.

6. Troesch, B. A., "Free Oscillations of a Fluid in a Container," Boundary Problems in Differential Equations, University of Wisconsin Press (1960), pp. 279-299.

7. Lawrence, H. R., Wang, C. J., and Reddy, R. B., "Variational Solution of Fuel Sloshing Modes" Jet Propulsion, 28, November 1958, pp. 729-736.

8. McLachlan, N. W., Bessel Functions for Engineers, Oxford University Press (1948).

9. Abramson, H. N., Dodge, F. T., and Kana, D. D., "Propellant Dynamic Problems in Space Shuttle Vehicles," NASA TM X-52876, Vol. II (1970), pp. 59-78.

10. Astleford, W. J., Chu, W. H., and Dodge, F. T., "Propellant Dynamic Problems in Space Shuttle Vehicles," Final Report, Part II, Contract NAS1-9890, Southwest Research Institute, October 1970.